913. Optimization of the rocket's nose and nozzle design parameters in respect to its aerodynamic characteristics

A. Fedaravičius[1], S. Kilikevičius[2], A. Survila[3]
Kaunas University of Technology, Kęstučio 27, 44025 Kaunas, Lithuania
E-mail: [1]*algimantas.fedaravicius@ktu.lt*, [2]*sigitas.kilikevicius@ktu.lt*, [3]*arvydas.survila@ktu.lt*
(Received 11 November 2012; accepted 4 December 2012)

Abstract. The airflow around rockets with various nose cone and nozzle cone geometric parameters is investigated in this paper. The mathematical background and the computational model of airflow around the rocket are designed for that purpose. ANSYS CFX computer modeling software is used to compute the airflow velocities, pressure, airflow turbulence kinetic energy, drag force and drag coefficient dependencies on rocket flight velocity. Optimization of the rocket's nose cone and nozzle cone geometry in respect to qualitative and quantitative parameters of rocket's aerodynamic characteristics is performed.

Keywords: ANSYS CFX, airflow, drag force, drag coefficient, Mach number, rocket.

Introduction

The geometrical and construction parameters and characteristics of exterior ballistics of a rocket are usually preset for a concrete rocket design. The range of rocket's velocities can be rather wide. The present design required developing a rocket which length is 5 meters and the diameter is 0.4 meters at speeds of the aerodynamic airflow less than 250 m/s. It is known that airflow characteristics and its parameters – airflow velocity, pressure, and turbulence kinetic energy – have a great influence on the exterior ballistics of the rocket. But the drag force and drag coefficient are the most important parameters necessary for the investigation of exterior ballistics – the necessary rocket engine thrust characteristics are directly related to these parameters.

The main objective of this paper is to identify an optimal configuration of five types of nose cones and a nozzle cone by computational modeling of the aerodynamic airflow, drag force and drag coefficient characteristics of the rockets in the velocity range of 0.3-0.8 Mach number.

Mathematical background

The airflow around the rockets has been modelled using the commercial finite element software ANSYS CFX. The set of equations solved by ANSYS CFX are the unsteady Navier-Stokes equations in their conservation form [1]:

(i) The continuity equation:

$$\frac{\partial \rho}{\partial t} + \nabla \cdot \left(\rho U \right) = 0, \tag{1}$$

where ρ is the density, U is the vector of velocity.

(ii) The momentum equations:

$$\frac{\partial \left(\rho U \right)}{\partial t} + \nabla \cdot \left(\rho U \otimes U \right) = -\nabla p + \nabla \cdot \tau + S_M, \tag{2}$$

where p is the pressure, S_M is the momentum source, τ is the stress tensor, which is related to the strain rate by:

$$\tau = \mu\left(\nabla U + (\nabla U)^T - \frac{2}{3}\delta\nabla\cdot U\right), \tag{3}$$

where δ is the Kronecker delta function (identity matrix), μ is molecular (dynamic) viscosity.

(iii) The total energy equation:

$$\frac{\partial(\rho h_{tot})}{\partial t} - \frac{\partial p}{t} + \nabla\cdot(\rho U h_{tot}) = \nabla(\lambda\nabla T) + \nabla\cdot(U\cdot\tau) + U\cdot S_M + S_E, \tag{4}$$

where h_{tot} is the total enthalpy, related to the static enthalpy $h(T, p)$ by:

$$h_{tot} = h + \frac{1}{2}U^2, \tag{5}$$

where λ is thermal conductivity, T is temperature, S_E is the energy source.

For turbulent flows the instantaneous equations are averaged leading to additional terms. However, the averaging procedure introduces additional unknown terms containing products of the fluctuating quantities, which act like additional stresses in the fluid. These terms called Reynolds stresses need to be modelled by additional equations. These equations define the type of turbulence model [1].

In this study the shear stress transport (SST) turbulence model was applied which is the most suitable for aeronautics flows with strong adverse pressure gradients and separation. The model (written in conservation form) is given by the following [2]:

$$\frac{\partial(\rho k)}{\partial t} + \frac{\partial(\rho U_i k)}{\partial x_i} = \tilde{P}_k - \beta^*\rho k\omega + \frac{\partial}{\partial x_i}\left[(\mu + \sigma_k\mu_t)\frac{\partial k}{\partial x_i}\right], \tag{6}$$

$$\frac{\partial(\rho\omega)}{\partial t} + \frac{\partial(\rho U_i\omega)}{\partial x_i} = \alpha\rho S^2 - \beta\rho\omega^2 + \frac{\partial}{\partial x_i}\left[(\mu + \sigma_\omega\mu_t)\frac{\partial\omega}{\partial x_i}\right] + \\ +2(1-F_1)\rho\sigma_{w2}\frac{1}{\omega}\frac{\partial k}{\partial x_i}\frac{\partial\omega}{\partial x_i}, \tag{7}$$

where k is the turbulence kinetic energy, ω is the turbulence frequency, μ_t is the turbulent viscosity. Blending function F_1 is defined by:

$$F_1 = \tanh\left\{\left\{\min\left[\max\left(\frac{\sqrt{k}}{\beta^*\omega y}, \frac{500v}{y^2\omega}\right), \frac{4\rho\sigma_{\omega 2}k}{CD_{k\omega}y^2}\right]\right\}^4\right\}, \tag{8}$$

where y is the distance from the field point to the nearest wall,

$$CD_{k\omega} = \max\left(2\rho\sigma_{\omega 2}\frac{1}{\omega}\frac{\partial k}{\partial x_i}\frac{\partial\omega}{\partial x_i}, 10^{-10}\right). \tag{9}$$

F_1 is equal to zero away from the surface (k-ε model), and switches over to one inside the boundary layer (k-ω model).

The turbulent eddy viscosity is defined as follows:

$$v_t = \frac{a_1 k}{\max\left(a_1\omega, SF_2\right)}, \tag{10}$$

where $v_t = \mu_y / \rho$, S is the invariant measure of the strain rate and F_2 is a second blending function:

$$F_2 = \tanh\left\{\left[\max\left(\frac{2\sqrt{k}}{\beta^*\omega y}, \frac{500v}{y^2\omega}\right)\right]^2\right\}. \tag{11}$$

A production limiter is used in the SST model to prevent the build-up of turbulence in stagnation regions:

$$P_k = \mu_t \frac{\partial U_i}{\partial x_j}\left(\frac{\partial U_i}{\partial x_j} + \frac{\partial U_j}{\partial x_i}\right) \rightarrow \tilde{P}_k = \min\left(P_k, 10\cdot\beta^*\rho k\omega\right). \tag{12}$$

The constants for the SST model are: $a_1 = 0.31$, $\beta^* = 0.09$, $\alpha_1 = 5/9$, $\beta_1 = 3/40$, $\sigma_{k1} = 0.85$, $\sigma_{\omega 1} = 0.5$, $\alpha_2 = 0.44$, $\beta_2 = 0.0828$, $\sigma_{k2} = 1$, $\sigma_{\omega 2} = 0.856$.

Computational model of airflow around the rocket

Five different rockets designs with different lengths of a parabolic nose cone were investigated (Fig. 1). The diameter of all rockets is 0.4 m. The rocket "A" (Fig. 1a) does not have a nozzle cone at the end; its length is 5 m. The lengths of the rockets with nozzle cones are 5.2 m. The diameter of the nozzle cone end is 0.15 m. The lengths of the nose cone are: 0.6 m for the rocket "B" (Fig. 1b), 0.8 m for the rocket "C" (Fig. 1c), 1 m for the rocket "D" (Fig. 1d), 2 m for the rocket "E" (Fig. 1e). The overall dimension between the fins is 1.6 m.

Three dimensional models of computational domains for the rockets were produced in SolidWorks software and imported into ANSYS CFX software. Computational numerical finite element models for a numerical simulation of airflow around the rockets were generated in ANSYS CFX software. Only a half of each model is discretized with the symmetric boundary condition in order to save computational time. The overall dimensions of the computational domain are 23.5 m in length and 3.5 m in radius.

The computational domain for each rocket was meshed using ANSYS CFX mesher. The maximal size of tetrahedral elements in the mesh was set to 150 mm and the maximal face size to 150 mm. In order to ensure the precision of results, 20 inflation layers were created on the surface of the rocket. These layers consist of prism elements. The first layer height was set to 2 mm and the growth rate to 1.1. On the surface of the rocket the mesh was made distinctly denser, the size of prism elements was set to 10 mm. The mesh with the quantity of 3.9 million elements containing tetrahedral and prism elements was generated for the simulation (Fig. 2).

As boundary conditions it was defined that the surface of the rocket is a non-slippery but smooth wall. The outside walls of the wind tunnel are defined as free slip walls. At the inlet air velocity is set at m/s. The Mach number of the flow for each rocket was changed from 0.3 to 0.8 during the simulation. At the outlet the relative static pressure was set to 0. Air temperature is 15° C and the reference pressure is 101325 Pa.

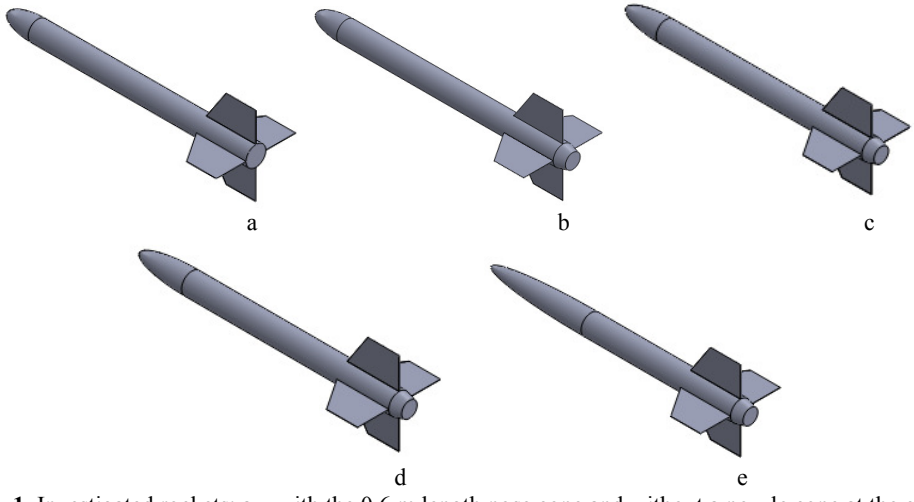

Fig. 1. Investigated rockets: a – with the 0.6 m length nose cone and without a nozzle cone at the end; b – with the 0.6 m length nose cone; c – with the 0.8 m length nose cone; d – with the 1.2 m length nose cone; e – with the 2 m length nose cone

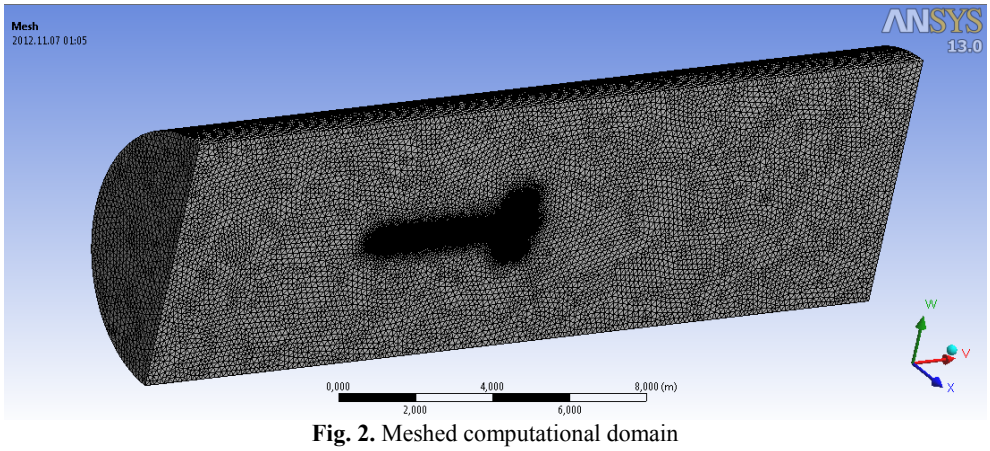

Fig. 2. Meshed computational domain

Results of the airflow simulation

Results of the simulation of airflow around the rockets were obtained.

The airflow velocity distribution on the cross-section plane, when the Mach number is 0.8, for the rocket "A" is shown in (Fig. 3a) and for the rocket "B" which has the nozzle cone at the end and the 0.6 m length nose cone in (Fig. 3b).

Velocity streamlines for the rockets are shown in Fig. 4 (the local values of velocity are shown in the streamlines' legends).

Pressure distribution contours, when the Mach number is 0.8, for the rocket "A" are shown in (Fig. 5a) and for the rocket "B" are shown in (Fig. 5b). The maximal value of pressure is a little bit higher for the rocket "A".

A significant increase of the turbulence kinetic energy can be observed when the rocket does not have a nozzle cone (Fig. 6). The maximum value of the turbulence kinetic energy for the rocket "B" with the nozzle cone (Fig. 6b) is about 63 % lower than for the rocket "A" (Fig. 6a).

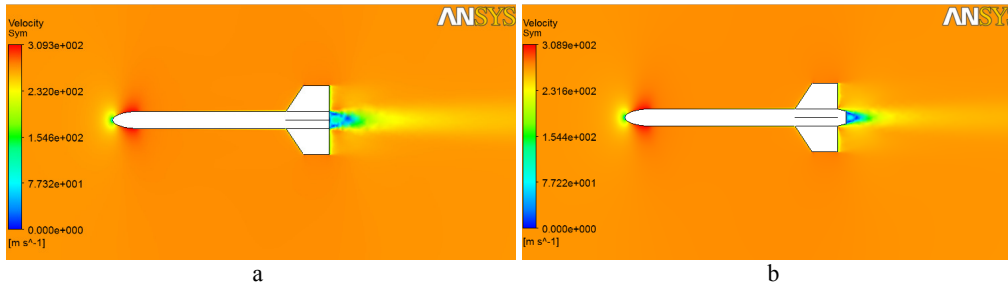

a b

Fig. 3. Velocity distribution on the cross-section plane when $M = 0.8$:
a – the rocket "A"; b – the rocket "B"

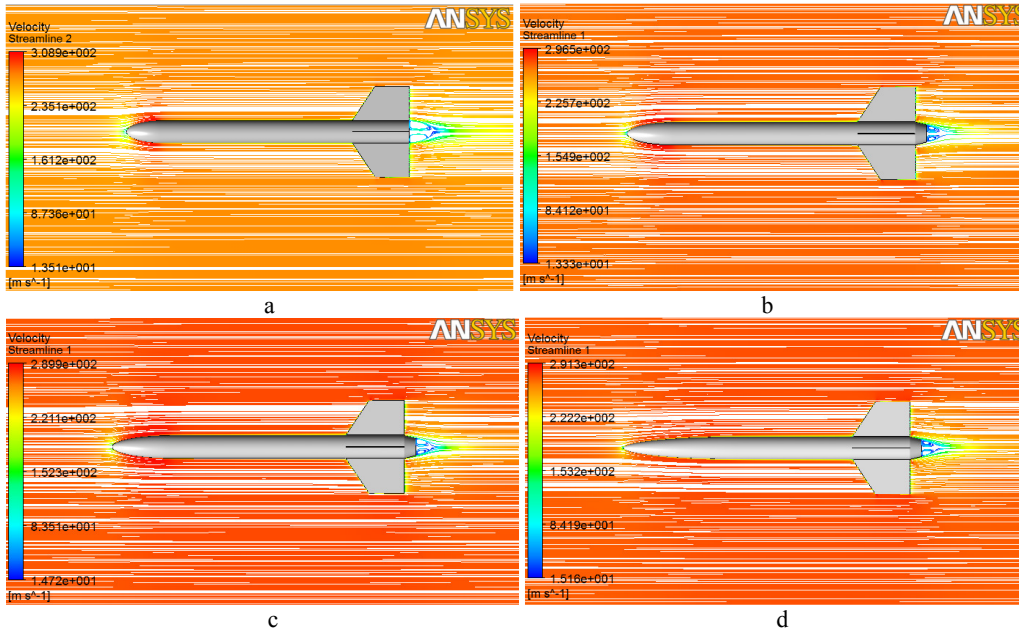

a b

c d

Fig. 4. Velocity streamlines on the cross-section plane when $M = 0.8$:
a – the rocket "A"; b – the rocket "C"; c – the rocket "D"; d – the rocket "E"

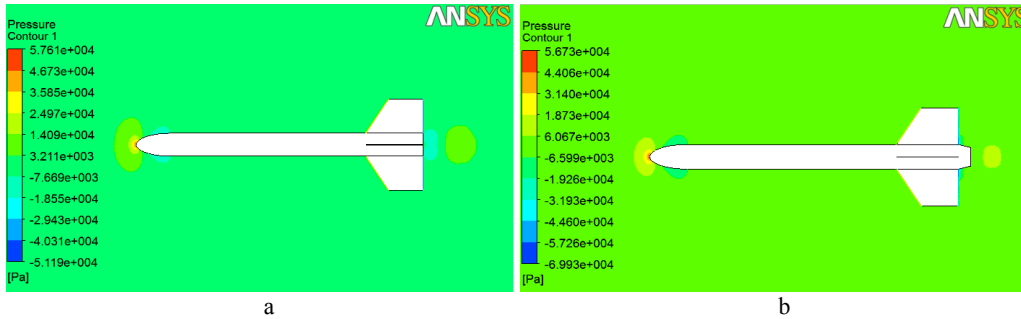

a b

Fig. 5. Pressure distribution when $M = 0.8$: a – the rocket "A"; b – the rocket "B"

The drag coefficient of the rockets was calculated by the following equation [3]:

$$C_d = \frac{F_d}{0.5\rho U^2 A}, \tag{13}$$

where F_d is the drag force, obtained from the simulation results; ρ is the air density; U is the velocity of airflow; A is the reference area. The calculated drag force of the rocket "B" with the nozzle cone is significantly lower compared to the drag force of the rocket "A" (Fig 7a). Accordingly, the drag coefficient of the rocket "B" is also from 27 % (at M = 0.3) to 29 % (at M = 0.9) lower compared to the drag coefficient of the rocket "A" (Fig 7b).

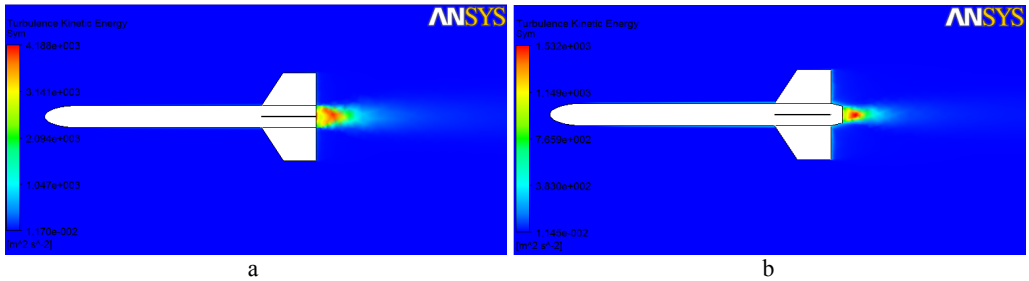

a b

Fig. 6. Turbulence kinetic energy when M = 0.8: a – the rocket "A"; b – the rocket "B"

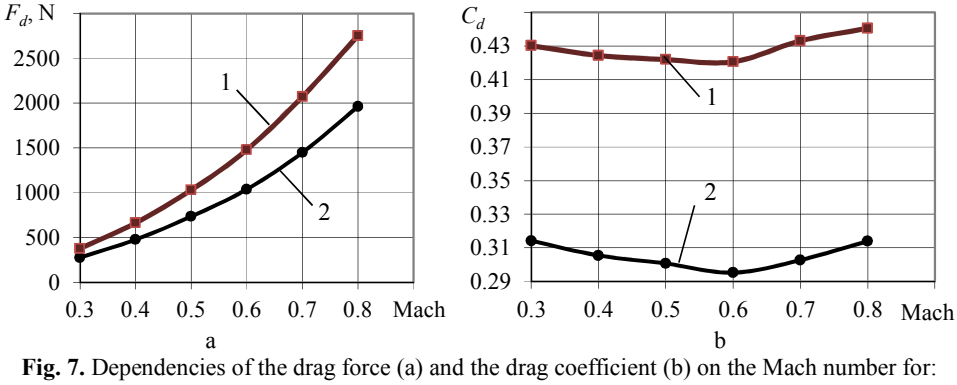

a b

Fig. 7. Dependencies of the drag force (a) and the drag coefficient (b) on the Mach number for:
1 – the rocket "A"; 2 – the rocket "B"

The simulation showed that the drag coefficients of the rockets "B", "C", "D", "E" do not vary significantly. The variation is within 5 % (Fig. 8).

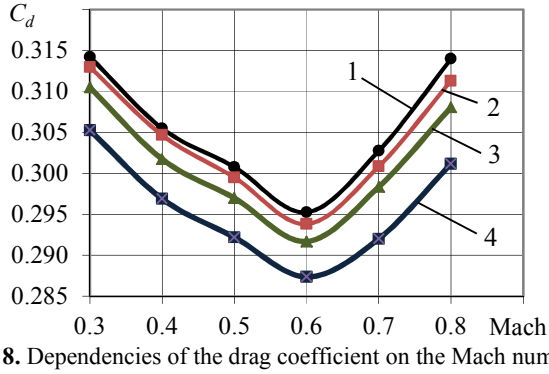

Fig. 8. Dependencies of the drag coefficient on the Mach number:
1 – the rocket "B"; 2 – the rocket "C"; 3 – the rocket "D"; 4 – the rocket "E"

Conclusions

An airflow simulation around four rockets with a different length of a parabolic nose cone and one rocket without a nozzle cone was performed. It was determined that there is a significant increase of the turbulence kinetic energy when the rocket does not have a nozzle cone. The maximum value of the turbulence kinetic energy for the rocket with the nozzle cone was about 63 % lower than for the rocket without it.

The calculated drag force of the rocket with the nozzle cone is significantly lower compared to the drag force of the rocket without it. The drag coefficient of the rocket with the nozzle cone is from 27 % (at $M = 0.3$) to 29 % (at $M = 0.9$) lower compared to the drag coefficient of the rocket without it. The nose cone length does not have a high influence on the drag coefficient for the rockets with the nose cone. The variation of the calculated drag coefficient of the rockets with different lengths of the nose cone was within 5 %.

References

[1] ANSYS CFX-Solver Theory Guide. ANSYS, Inc., Southpointe 275 Technology Drive Canonsburg, PA 15317: 23–96.

[2] Menter F. R., Kuntz M., Langtry R. Ten years of industrial experience with the SST turbulence model. Turbulence, Heat and Mass Transfer 4, Ed: K. Hanjalic, Y. Nagano and M. Tummers, Begell House, Inc., 2003, p. 625 – 632.

[3] Mills A. F., Irwin R. D. Basic Heat and Mass Transfer. University of California at Los Angeles, 1995, p. 254 – 921.

[4] Fedaravičius Algimantas, Jonevičius Vaclovas, Kilikevičius Sigitas, Paukštaitis Linas, Šaulys Povilas Estimation of the drag coefficient of mine imitator in longitudinal air flow using numerical methods. Transport, Vilnius: Technika, Taylor&Francis, Vol. 26, No. 2, 2011, p. 166 – 170.